



Study on supercapacitance performance of TiO₂ nanotube arrays modified by non-metal doping and Polyaniline electrodeposition methods

Mehri Maghsoudi, Shahin Khameneh Asl*, Faezeh gorbani

Department of Materials Engineering, Faculty of Mechanical Engineering, University of Tabriz, Tabriz, Iran.

Received: 20 February 2021; Accepted: 29 April 2021

* Corresponding author email: khameneh@tabrizu.ac.ir

ABSTRACT

Highly ordered TiO₂ nanotube arrays were synthesized by a two-step anodizing method. Providing unidirectional path for electron transfer, led TiO₂ nanotubes to have excellent electrical and capacitive properties. But these properties can be improved by effective methods such as non-metallic doping or by a conductive polymer. For this purpose, nitrogen and hydrogen doping methods and electrical deposition of polyaniline were used simultaneously to prepare the polyaniline-TiO₂, polyaniline/N-TiO₂, and polyaniline/H-TiO₂ nanotube arrays samples. To evaluate the electrochemical and capacitive properties in more detail, cyclic voltammetry, electrochemical impedance spectroscopy, Mott-Schottky, and galvanostatic charge-discharge tests were performed. The results showed that the composite of TiO₂ doped with hydrogen and deposited with polyaniline nanowires had the highest capacitance (5666 μF.Cm⁻²) at the current density of 100 μA/cm², approximately 4.5 times more than polyaniline/TiO₂ sample. It also has the lowest charge transfer resistance (0.008 Ωcm²) and the highest charge carrier density (1.63×10²⁴cm⁻³). Increasing the density of charge carriers and decreasing the electrical resistance can be attributed to the fact that the hydrogen doping, the presence of oxygen vacancies, and conductive polymer can increase the rate of separation of the charge carriers and decrease their recombination rate. Therefore, the electron transfer rate and the electric current increase.

Keywords: TiO₂ nanotube arrays, Non-metal doping, Polyaniline, EIS, Capacitive performance.

1. Introduction

Electrochemical energy storage is one of the most important candidates for resolving the non-renewable energy crisis. As a result, attention has shifted to renewable-energy storage devices, including supercapacitors [1]. Supercapacitors (or electrochemical capacitors) have advantages such as high power density, fast charge-discharge capability, and long cycling life [2]. According to the storage mechanism, supercapacitors can be classified into two groups. The first group is electric double-layer

capacitors, which include materials such as carbon materials (carbon nanotubes, graphene, etc.). The next group is pseudocapacitor, which includes materials such as oxides of intermediate metals (such as TiO₂, RuO₂ oxide, etc.) and conductive polymers (polyaniline and polypyrrole, etc.) [3]. The charge in the pseudocapacitors often stores through rapid and reversible oxidation-reduction reactions. Whereas in electric double-layer capacitors, the charge storage is based on the electrostatic charge penetration and its accumulation at the interface

between the electrode and the electrolyte [2, 4]. One of the most important and effective components of superconductors is the electrode. The properties of the materials used in the electrodes of the supercapacitors greatly influence the performance of the supercapacitors. Therefore, over the past years, extensive researches have been done to optimize and increase the efficiency of electrode materials [5, 6]. Among the various metal oxides, titanium oxide is one of the most suitable materials for supercapacitor electrodes due to its mechanical strength, environmental stability, excellent charge transfer properties, and low synthesis cost. Among the different morphologies of titanium oxide, nanotube arrays have been further studied for providing one-way and direct paths for electron transfer [7]. Although TiO_2 nanotubes have excellent electrochemical properties, due to their semiconductive nature and wide bandgap, they have poor electrical conductivity and capacitive behavior without any modification. Therefore, different methods such as heat treatment, metal or non-metal doping, decoration with noble metal particles, and synthesis of nanocomposites with electronically active materials such as conductive polymer can increase the capacitance of TiO_2 nanotubes [8, 9]. Among these methods, non-metallic doping, especially nitrogen and hydrogen, is a facile and effective method. By the non-metallic element doping, electron donor states are created in the titanium oxide bandgap. Hence charge carriers density and electrical conductivity of titanium oxide are increased [10, 11]. Wu et al. used a simple hydrogenation doping method to significantly improve the electronic conductivity and the capacitive performance of TiO_2 nanotube electrodes. These electrodes treated by the electrochemical hydrogenation doping. The modified electrodes display a high average specific capacitance of $20.08 \text{ mF}\cdot\text{cm}^{-2}$ at a current density of 0.05 mA cm^{-2} , ~ 20 times more than the pristine TiO_2 nanotube electrodes [12]. In another study, Samsudin et al. in order to modification of the TNTs, applied a fast and facile electrochemical reduction method. R-TNTs that prepared at 5V for 30 s had a specific capacitance of $11.12 \text{ mF}\cdot\text{cm}^{-2}$ at a current density of $20 \text{ }\mu\text{A}\cdot\text{cm}^{-2}$ [13]. Among conductive polymers, polyaniline (PANI) has received much attention due to its unique properties such as different oxidation modes, environmental stability, and good electron activity. Polyaniline has three different forms depending

on the degree of oxidation. The leucomeraldine base refers to the fully reduced polyaniline state. Whereas emeraldine base is a half-oxidized form, and pernigraniline is completely oxidized. The only conductive form of polyaniline is emeraldine salt, which is obtained by doping or protonation of the base. These forms of polyaniline are easily converted. Transitions between different forms of polyaniline are accompanied by changes in color and conductivity [14, 15]. Polyaniline is obtained by chemical or electrochemical polymerization of aniline. The electrochemical polymerization method is desirable because the polymer is directly deposited on the electrode surface and facilitates analysis. This method has other advantages than the chemical method, such as control of the thickness of the polymer deposition, low cost, and no need for a catalyst [16]. Xiao et al. prepared polyaniline/ TiO_2 nanotube arrays composite electrodes by depositing polyaniline on TiO_2 nanotube arrays through the cyclic voltammetry method. The areal capacitance of the composite electrode fabricated in ethanol solvent is $6.25 \text{ mF}\cdot\text{cm}^{-2}$ at the scan rate of 50 mV/s [17]. EIS and Mott-Schottky tests are two powerful and valuable tools for studying the electrochemical properties of materials, including TiO_2 nanotube arrays as a supercapacitor electrode. In previous articles, these tests, especially Mott-Schottky, have either not been performed or a brief explanation has been provided. Also, similar works have investigated the properties of titanium oxide nanotubes doped with non-metallic elements such as nitrogen (N- TiO_2 NTAs) and hydrogen (H- TiO_2 NTAs) or polyaniline/ TiO_2 NTAs. While the electrochemical properties and capacitive performance of the Polyaniline/N- TiO_2 NTAs and polyaniline/H- TiO_2 NTAs have not been fully investigated [13, 17-21]. In this paper, we tried to examine the electrochemical properties of samples in more detail using these tests. Due to the simultaneous effect of hydrogenation doping (creating of oxygen vacancy) and PANI electrodeposition (PANI/H- TiO_2 NTs electrode), the result of Mott-Schottky indicates that most charge carrier density ($1.63 \times 10^{24} \text{ cm}^{-3}$) and the least charging transfer resistance ($0.008 \text{ }\Omega\cdot\text{cm}^2$). In this study, the two-step anodic oxidation method was used for the synthesis of well-aligned TiO_2 nanotubes. To compare the effect of different dopants, the samples were doped once with nitrogen by immersion in ammonia and once again, using the two-electrode system,

the samples were doped with hydrogen. Finally, the polyaniline nanowires were deposited on the nanotubes by electrochemical polymerization. Cyclic voltammetry, electrochemical impedance spectroscopy, Mott-Schottky, and galvanostatic charge-discharge performed to evaluate the electrochemical properties and supercapacitive performance of the samples.

2. Materials and Methods

2.1 Preparation of TiO₂ nanotube arrays

In this study, for sample preparing, grade 2 titanium sheet with 99.7% purity and 0.5 mm thickness was cut into 1×2 cm pieces. To achieve regular and smooth nanotubes at anodizing, the substrate must be smooth and clear. For this purpose, the samples were first sanded with sandpaper from 220 to 2000 mesh and then polished with 0.5 μm alumina powder to achieve mirror-like surfaces. Then the samples were subjected to ultrasonic irradiation in acetone and ethanol for 15 min, respectively. Finally, the samples were washed with distilled water and thoroughly dried. The TiO₂ nanotube arrays were synthesized by the anodizing method. Anodizing was performed on a two-electrode system in which the prepared Ti sheet was used as the anode and the stainless steel sheet used as the cathode. The intermediate distance between two electrodes was 2 cm, and the electrolyte temperature was 28 °C. The anodizing electrolyte contained ethylene glycol, 0.15 M NH₄F, and 3% vol deionized water. The first anodizing was performed at 2h at a voltage of 60V. To obtain more regular and better adhesion to the substrate, the oxide layer formed by the first anodizing was ultrasonically removed in distilled water from the substrate. The second anodizing was then carried out in the same solution and condition and time of 3h. Finally, the samples were washed with distilled water and ethanol to remove residual organic electrolytes. To remove residual debris on the top surface of the nanotubes, the samples were ultrasonicated for 30 s in 50 nm alumina powder slurry and washed again with distilled water.

2.2 Preparation of N-TiO₂ and H-TiO₂ NTAs

The nanotubes prepared by anodizing were exposed to nitrogen doping. They were immersed in 2 M NH₃·H₂O solution for 15 h and then washed with deionized water and dried. Subsequently, because the primary nanotubes were amorphous, the doped samples (N-TiO₂) were annealed

at 500 °C for 4 h at a rate of 2.1 °C / min to obtain the crystalline structure in the ambient atmosphere. For hydrogenation of TiO₂ nanotubes, the samples were first annealed at 500 °C. The electrochemical hydrogenation of the nanotubes was then performed on a two-electrode system in 0.5M Na₂SO₄ solution. TiO₂ nanotube arrays had been used as cathode and graphite electrode as anode. Between the two electrodes, a 5 V voltage was applied for 30 seconds. During the process, hydrogen and oxygen were evolutioned on the cathode (TiO₂ nanotubes) and anode (graphite) surface, respectively. The doped samples (H-TiO₂) washed with deionized water and dried.

2.3 Preparation of PANI/N-TiO₂ and PANI/H-TiO₂ NTAs nanocomposites

The electrical deposition of polyaniline was performed on TiO₂, N-TiO₂ and, H-TiO₂ NTs samples in the three-electrode system. In this system, the saturated calomel electrode (SCE), platinum sheet and, the prepared samples were used as a reference, counter and working electrodes, respectively. The aqueous base electrolyte contained 0.5 M sulfuric acid + 0.1 M aniline monomer. Electrochemical polymerization was performed by cyclic voltammetry from -0.7 to 1V voltage at a scan rate of 200 mV/s for 30 cycles. After that, the samples rinsed with deionized water and dried. The color of the samples changed to green after the electrodeposition of polyaniline.

2.4 Characterization

The surface morphologies of PANI/TiO₂ NTs, PANI/N-TiO₂ NTs and, PANI/H-TiO₂ NTs were characterized by a field emission scanning electron microscope (FE-SEM, MIRA3 TESCAN) at an acceleration voltage of 10 kV. The crystallization of the prepared samples were determined by X-ray diffractometer (XRD, D-5000 Siemens with Cu Kα radiation). The FTIR spectrum was recorded over a wavenumber range of 400-4000 cm⁻¹ (FTIR-8400S.SHIMADZU). Cyclic Voltammetry (CV), electrochemical impedance spectroscopy (EIS), Mott-Schottky and Galvanostatic charge-discharge (GCD) were used to examine the electrochemical properties and capacitive performance using an electrochemical workstation (Wonatech, ZIVE SP1). The electrochemical tests were performed in a three-electrode system composed of the sample as the working electrode, the Pt sheet as the counter electrode, and the SCE as the reference electrode.

The electrolyte of electrochemical tests were conducted in 0.5M H₂SO₄. The frequency range was selected between 100 kHz to 0.01Hz with a 10mV amplitude for the EIS test. The Mott–Schottky method was performed at a single frequency of 1000Hz and a potential between -0.1 to 0.9V with a step potential of 0.05V to study the donor density on the electrode surface.

3. Results and discussion

Fig.1a depicts the top view of the FESEM image of TiO₂ nanotube arrays. As the result of two-step anodization, Well-ordered and uniform nanotubes with open top surface are synthesized. TiO₂ nanotubes have an inner diameter of approximately 129 nm and a wall thickness of 27-34 nm. Fig.1b shows the EDS spectrum of TiO₂ nanotube arrays. TiO₂ nanotubes contain the elements of Ti, O, N and C. The top view of the FESEM image of PANI/TiO₂ nanotube composite was presented in Fig.1c. As seen in Fig.1c, irregular PANI nanowires are formed on the top surface of TiO₂ nanotubes. Nonetheless, the regular morphology of TiO₂ nanotubes was maintained. Fig.1d shows the

EDS spectrum of PANI/TiO₂ nanotubes. Samples contain the elements of Ti, O, N, C and, S. High content of the Carbon element in the sample indicates that PANI nanowires have deposited successfully on the top surface of TiO₂ nanotubes. Electrochemical polymerization by CV method was used for Polyaniline deposition. Fig.2a shows CV curves recorded in cycles of 1,5,10,15,20,25 and 30 at scan rate of 200 mV/s. Redox peaks of aniline polymerization appeared in the CV voltammograms, indicating the existence of PANI. As shown in Fig.2a, when cycle number increases, anodic peak current (oxidation) also increases. In contrast, cathodic peak potential (reduction) slightly shifted toward a negative potential and oxidation potential shifted toward a positive potential. These results demonstrate facility of aniline electropolymerization and increase electropolymerization rate. As can see from Fig.2b, first anodic peak at potential 0.2 V corresponds with the transformation of Leucoemeraldine base (fully reduced form) to Emeraldine salt (half reduced form). Another anodic peak at potential 0.8 V refers to the transformation of Emeraldine

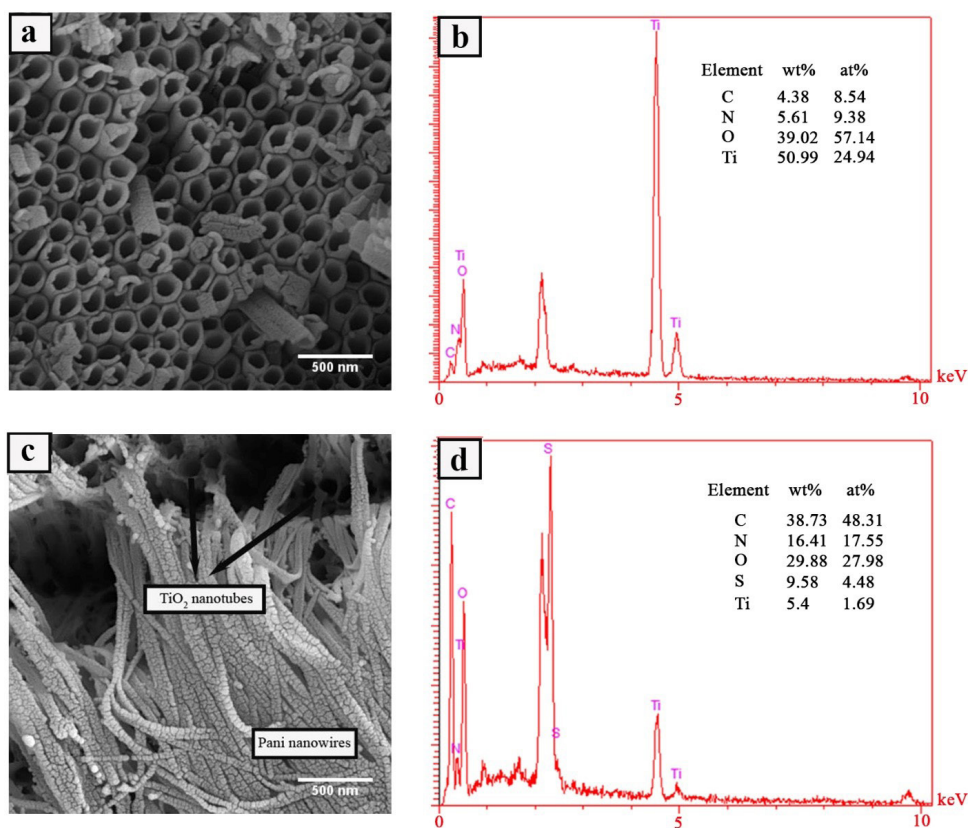


Fig. 1- Top view of FESEM images and EDS spectra of TiO₂ NTAs (a,b), PANI/TiO₂ NTAs (c,d).

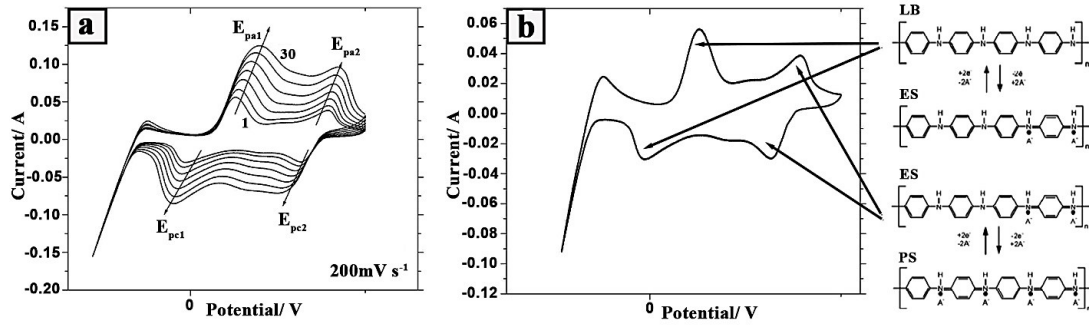


Fig. 2- curves of electrochemical polymerization of aniline by CV method at scan rate of 200 mV/s (a) and characteristic peaks in cyclic voltammograms of electrochemical polymerization (b).

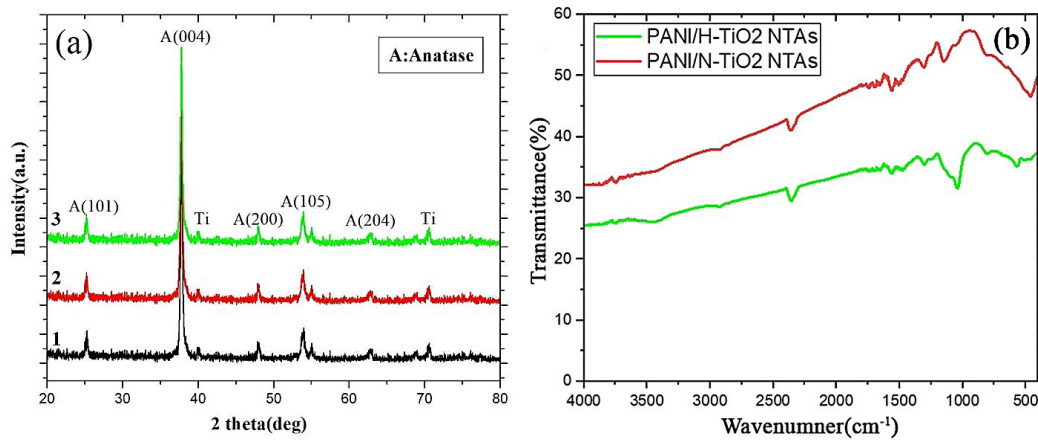


Fig. 3- (a) XRD patterns of 1: PANI/TiO₂ NTs, 2: PANI/N-TiO₂ NTs, 3: PANI/H-TiO₂ NTs and (b) FTIR spectra of PANI/N-TiO₂ NTs, PANI/H-TiO₂ NTs.

salt to the Pernigraniline base (fully oxidized) [22].

The XRD patterns of PANI/TiO₂, PANI/N-TiO₂, and PANI/H-TiO₂ NTs samples are illustrated in Fig.3a. The peaks at 25.3°, 37.8°, 48°, 54.2°, and 63° correspond to the (101), (004), (200), (105) and (204) diffraction peaks that can be attributed to Anatase TiO₂ (JCPD:21-1272). It can be deduced that the position and intensity of Anatase peaks didn't change due to non-metal doping and PANI electrodeposition. Therefore hydrogenation and nitrogen doping, as well as PANI electrodeposition, didn't affect the crystal structure of TiO₂ nanotubes [19].

Fig.3b shows the FTIR spectrum of PANI/N-TiO₂ and PANI/H-TiO₂ NTs. FTIR analysis was conducted to investigate the structural information of these samples and to confirm the formation of polyaniline and the doping of nitrogen and hydrogen. Several characteristic peaks are appeared on the FTIR spectra of samples at a wavenumber of 400-4000 cm⁻¹. The broad peak from 400 to 800 cm⁻¹ and 3200 to 3600 cm⁻¹ are assigned to Ti-O-Ti

stretching vibration and O-H stretching vibration on TiO₂ nanotubes, respectively. After immersing of TiO₂ NTAs in NH₃.H₂O solution, the new peak around 1451 cm⁻¹ is related to N-Ti-O stretching vibration [11]. Electrochemical hydrogenation doping of TiO₂ NTAs cause shift the absorption band of Ti-O-Ti [23]. After the electrodeposition of PANI, the main characteristic bands of PANI are attributed as follows: The band at 3440 cm⁻¹ is due to the N-H stretching mode. The peaks at 1490 cm⁻¹ and 1475 cm⁻¹ correspond to C=C stretching vibration in the benzenoid ring of PANI/N-TiO₂ and PANI/H-TiO₂, , respectively. The peaks at 1566 cm⁻¹ and 1564 cm⁻¹ correspond to C=C stretching vibration in the quinoid phenyl ring of PANI/N-TiO₂ and PANI/H-TiO₂ NTAs, respectively. For PANI/N-TiO₂ NTAs, the peaks at 1305 cm⁻¹ and 1240 cm⁻¹ are related to the C-N stretching vibration of the benzenoid unit. While, For PANI/H-TiO₂ NTAs, the peaks at 1307 cm⁻¹ and 1242 cm⁻¹ are related to the C-N stretching vibration of the benzenoid unit. The peak at 800 cm⁻¹ is attributed to

the stretching vibration of the C-C and C-H bonds in benzenoid ring. As a result, the presence of main peaks of polyaniline in the spectrums confirms the formation of polyaniline on the surface of titanium oxide nanotubes. However, due to the interaction of polyaniline with samples of titanium oxide nanotubes doped with nitrogen and hydrogen, the characteristic peaks of the samples are shifted [24, 25].

Fig.4a displays cyclic voltammetry curves of PANI/TiO₂, PANI/N-TiO₂, and PANI/H-TiO₂ NTs at a scan rate of 50 mV/s. As the figure shows, the current density of PANI/H-TiO₂ NTs is the highest, and the integrated inner area of the curve is the largest; therefore it is expected to enhance capacitance performance of PANI/H-TiO₂ NTs composite. To investigate the claim, the capacitance of samples calculated through the following equation and CV curves [26].

$$C_s = \left(\int IdV \right) / vSV \quad (1)$$

Where C_s is the areal capacitance (mF/cm²), I is

the current (A), v is the scan rate (V/s), V is the potential (V), and S is the surface area of the working electrode (cm²). The areal capacitance calculated for PANI/TiO₂, PANI/N-TiO₂, and PANI/H-TiO₂ NTs are 150, 223, and 287 mF/cm², respectively. These results indicate that hydrogenation doping and PANI electrodeposition can increase both conductivity and charge carriers. Nitrogenation also increases capacitance, but the effect of Hydrogenation is greater due to increased electron transfer rate. CV curves were recorded at different scan rates (10-200 mV/s) for PANI/H-TiO₂ NTs (Fig.4b). As seen in Figure, The shape of curves are retained with scan rate increases, so it exhibits good capacitance. Besides, with an increase of scan rate, oxidation peaks toward positive potentials, and reduction peaks toward negative potentials are shifted, showing good reversibility of PANI/H-TiO₂ NTs. The areal capacitance of samples in terms of the scan rate is presented in Fig.4c. The areal capacitance of samples is decreased with increasing the scan rate. The areal capacitance of PANI/H-TiO₂ NTs is decreased from 395 mF/cm² to 242 mF/cm²

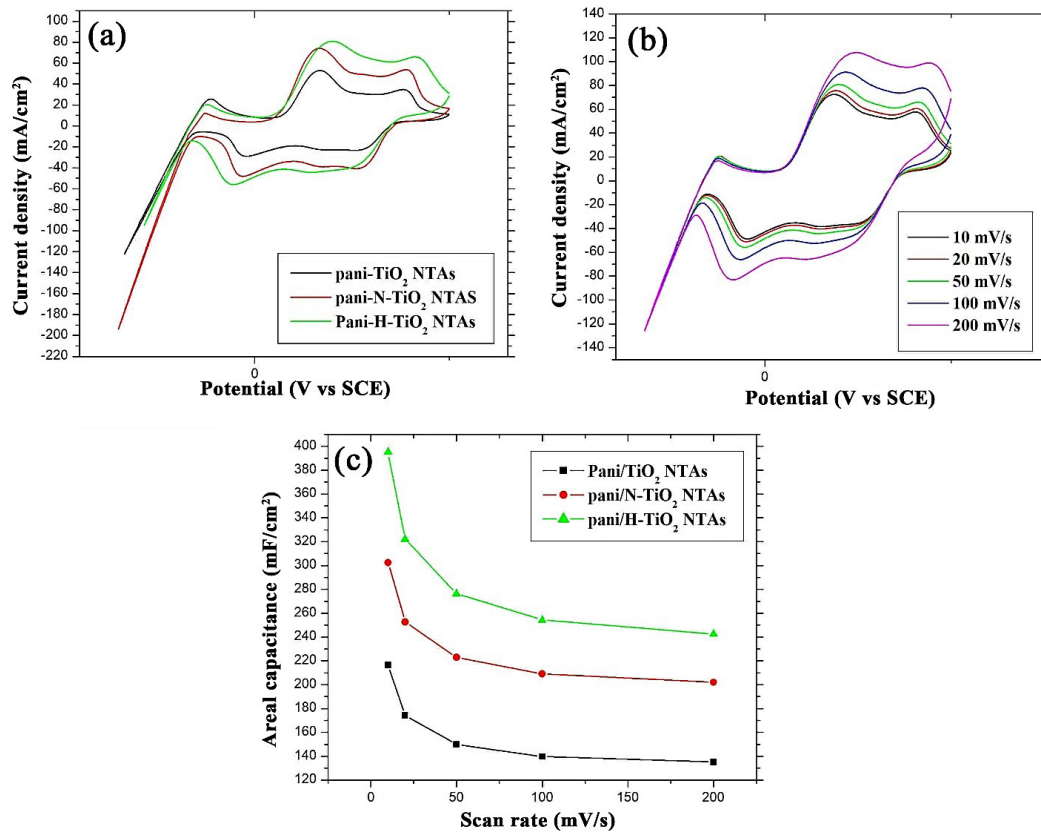


Fig. 4- CV curves of PANI/TiO₂, PANI/N-TiO₂, and PANI/H-TiO₂ NTs at the scan rate of 50 mV/s (a), CV curves of PANI/H-TiO₂ NTs recorded at different scan rate from 10 to 200 mV/s (b), the areal capacitance of samples in terms of different scan rate (c).

cm² with increasing the scan rate from 10 to 200 mV/s. 61.3% of the initial capacitance remained. At the same scan rate, the areal capacitance of PANI/H-TiO₂ NTs is higher than other samples. Modification processes such as hydrogen doping accompanied by PANI electrodeposition cause improve charge carriers transport significantly, so enhance electrical conductivity [21].

The Nyquist plots of PANI/TiO₂, PANI/N-

TiO₂, and PANI/H-TiO₂ NTs have been shown in Fig.5a-c. As seen from Figure, the plots contain two semicircles that one is in the high frequency, and the other is in the low-frequency region. The enlarged high-frequency segment has been shown in the inset of the figure. In this electrochemical system, we considered two interfaces between electrolyte/PANI nanowires and between PANI nanowires/TiO₂ nanotubes. Therefore, the equivalent circuit

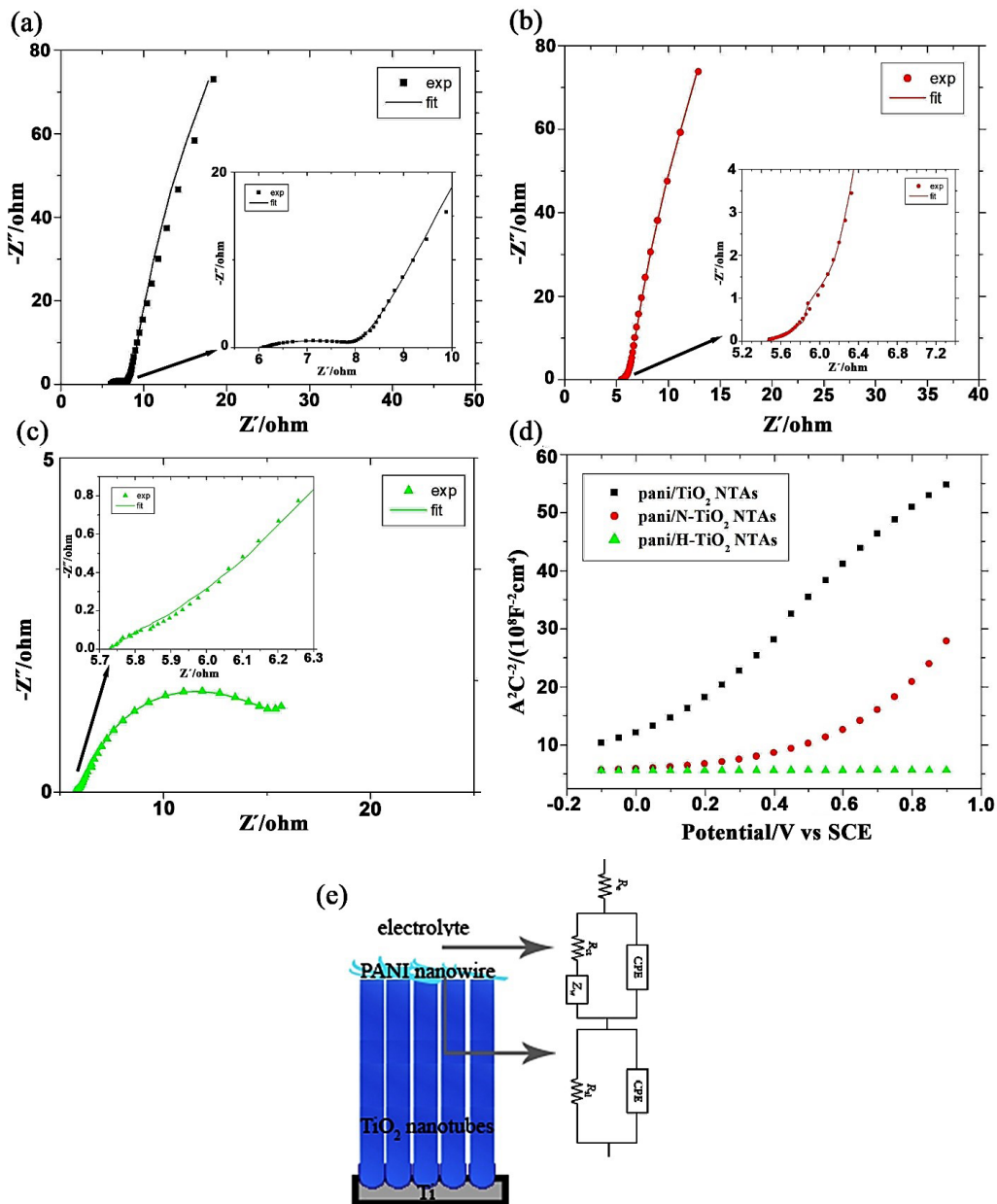


Fig. 5- The Nyquist plots of PANI/TiO₂ (a), PANI/N-TiO₂ (b), PANI/H-TiO₂ NTs (c) in a frequency range of 100 kHz-10 MHz with 10mV amplitude in a 0.5M H₂SO₄ solution, the Mott-Schottky plot of electrodes in a frequency of 1000Hz with a potential range of -0.1V to 0.9 V (d) and electrical equivalent circuit for impedance spectra fitting (e).

Table 1- Fit parameters of the equivalent circuit for the Nyquist plots shown in Fig.5

Element	PANI/TiO ₂ NTs	PANI/N-TiO ₂ NTs	PANI/H-TiO ₂ NTs
R _s (Ω.cm ²)	6.12	5.45	5.73
CPE _{dl} -T(mF.cm ⁻²)	0.136	0.219	0.303
CPE _{dl} -P(mF.cm ⁻²)	0.82	0.16	0.74
R _{ct} (Ωcm ²)	1.9	0.02	0.008
W-R(Ω.cm ²)	3.55	1.29	0.31
W-T(S.s ^{-0.5})	0.004	0.03	0.06
W-P	0.39	0.72	0.19
CPE _c -T(mF.cm ⁻²)	0.002	0.005	0.006
CPE _c -P(mF.cm ⁻²)	0.99	0.97	0.95
R _c (Ωcm ²)	35.93	23.45	7.108

of Fig.5e was used to fit the electrochemical impedance data with ZView software, and the fitting results are presented in Table1. R_s is the solution, and connections resistance, R_{ct} related to charging transfer resistance and CPE_{dl} is the double layer capacitance in between electrode/electrolyte interface. The phenomenon of ions diffusion in the interface of electrode and electrolyte are illustrated with the Warburg element. The low-frequency semicircle is related to the interface between PANI nanowires and TiO₂ nanotubes. As can be inferred from the Fig.5 and Table.1, the charge transfer resistance of the interface in PANI/H-TiO₂ NTs is the least; indicating increase in the rate of separation and transfer of charges. As the result, the electric current increases. In addition, Warburg resistance and contact resistance are much lower and CPE_{dl} is higher for PANI/H-TiO₂ NTs [21]. To further investigation of the electrochemical properties of the samples as a supercapacitor electrode, Mott-Schottky plots recorded at a frequency of 1000 Hz (Fig.5d). The following formula calculates the carrier density (N_D).

$$\frac{1}{C_{sc}^2} = \frac{2}{\epsilon\epsilon_0 e N_D} \left(E - E_{fb} - \frac{KT}{e} \right) \quad (2)$$

Where ε is the dielectric constant of the semiconductor (for anatase: 31), ε₀ is vacuum permittivity (8.854 × 10⁻¹⁴ F/cm), e is the electron charge (1.602 × 10⁻¹⁹ C), E is applied potential, K is the Boltzmann constant, T is the absolute temperature, N_D displays the donor density and C_{sc} designates the capacitance of the space charge [27]. As can be inferred from the Fig.5 and Table.2, the N_D for PANI/H-TiO₂ NTs is much higher than PANI/N-TiO₂ and PANI/TiO₂. The result of Mott-Schottky indicates that charge carrier density and rate of charge transfer were enhanced. All these results prove that the PANI/H-TiO₂ NTs electrode has better capacitive performance due to

Table 2- Parameters of Mott-Schottky plot

Sample	N _D (cm ⁻³)	E _b (V)
PANI/TiO ₂ NTs	7.9×10 ²⁰ cm ⁻³	0.05
PANI/N-TiO ₂ NTs	1.45×10 ²¹ cm ⁻³	0.5
PANI/H-TiO ₂ NTs	1.63×10 ²⁴ cm ⁻³	-

the simultaneous effect of hydrogenation doping and PANI electrodeposition which, increase the capacitance.

The galvanostatic charge-discharge test assesses the capacitive performance of electrodes. Fig.6a shows the charge-discharge curves of electrodes at the current density of 100μA/cm². As shown in Figure, curves of potential in terms of time during the charge-discharge process have a slightly non-linear shape that indicates a reversible and fast Faradic process. Areal capacitance is calculated by the following formula [28].

$$C_s = I\Delta t/S\Delta V \quad (3)$$

Where C_s is the areal capacitance (μA/cm²), I is the constant current during discharge (A), ΔT is the discharge duration (s), ΔV is the potential window (V), and S is the surface area of the electrode (cm²). The areal capacitance of PANI/TiO₂, PANI/N-TiO₂, and PANI/H-TiO₂ NTs are 1250, 1417, and 5666 μF/cm², respectively. It can be inferred from the increased capacitance that its reason is the existence of Nitrogen and Hydrogen dopants. Non-metal doping is an easy and inexpensive method that helps rapid charge transfer and enhances the charge carriers and reduces the recombination rate. So the electrical current and consequently capacitance will enhance. The effect of Hydrogen doping is greater than Nitrogen doping because it facilitates the faster transfer of charge and increases the electrical current, due to interstitial hydrogen ions and oxygen vacancy [29]. However, nitrogen is also known to be an effective doping agent because

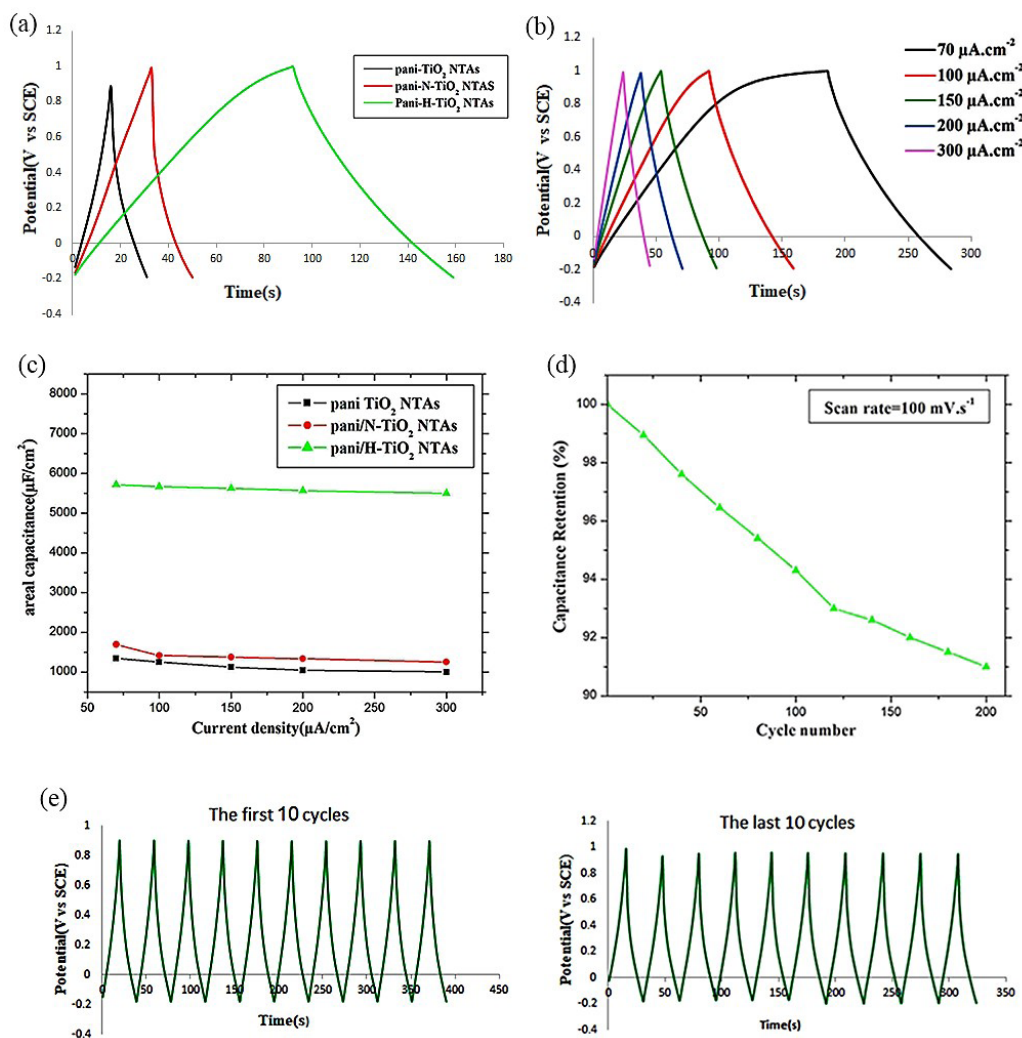


Fig. 6- Galvanostatic charge-discharge curves of prepared electrodes at a current density of $100\mu\text{A}/\text{cm}^2$ (a), galvanostatic charge-discharge curves of PANI/H-TiO₂ NTs at different current density from 70 to $300\mu\text{A}/\text{cm}^2$ (b), the areal capacitance in terms of current density for electrodes.

it exhibits better electrochemical and capacitive performance than non-doped samples [30]. The electrodeposition of conductive polymer such as Polyaniline on the surface of TiO₂ nanotubes is another useful and efficient method. PANI electrodeposition significantly improves electrical conductivity and capacitive performance. Fig.6b presents the charge-discharge curves of PANI/H-TiO₂ NTs at various current density from 70-300 $\mu\text{A}/\text{cm}^2$. As the current density enhances from 70 to 300 $\mu\text{A}/\text{cm}^2$, the areal capacitance of samples is slightly reduced (Fig.6c). In every current density, the areal capacitance of PANI/H-TiO₂ NTs is much higher than other samples. The capacitive stability test was performed on the optimal sample during 200 cycles. The first ten and the last ten

cycles, together with the capacitance retention, are shown in Fig.6d. As can be seen from figure.6d, its capacitive stability is not significant. Because the prepared electrode is a pseudocapacitor electrode, the pseudocapacitors have lower cyclic stability despite their high capacitance. It is worth mentioning that to increase the stability and cyclic life of the PANI/H-TiO₂ NTs electrode, it should be combined with an electric double-layer capacitor type to form a composite.

4. Conclusion

Titanium oxide nanotubes are recognized as one of the most suitable candidates for capable electrochemical capacitors by providing direct and one-dimensional paths for fast charge transfer and

high surface area. But because of the semiconductor nature and the large energy band gap, it has to be composed of electronically active materials. In this paper, titanium nanotubes effectively doped with non-metallic elements (nitrogen and hydrogen). Then, to further increase the electrical conductivity, the polyaniline nanowires were electrically deposited on the doped nanotubes. The results showed that the composite of TiO₂ doped with hydrogen and deposited with polyaniline nanowires had the highest capacitance (5666 μF.Cm⁻²) at the current density of 100 μA/cm², approximately 4.5 times more than PANI/TiO₂ sample (1250 μF.Cm⁻²). It also has the lowest charge transfer resistance (0.008 Ωcm²) and the highest charge carrier density (1.63×10²⁴cm⁻³). Non-metal doping helps rapid charge transfer and enhances the charge carriers and reduces the recombination rate. So the electrical current and consequently capacitance will enhance. The effect of Hydrogen doping is more significant than Nitrogen doping because it facilitates the faster transfer of charge and increases the electrical current, due to interstitial hydrogen ions and oxygen vacancy.

References

1. Miller JR, Simon P. MATERIALS SCIENCE: Electrochemical Capacitors for Energy Management. *Science*. 2008;321(5889):651-2.
2. Kötz R, Carlen M. Principles and applications of electrochemical capacitors. *Electrochimica Acta*. 2000;45(15-16):2483-98.
3. Wang Y, Song Y, Xia Y. Electrochemical capacitors: mechanism, materials, systems, characterization and applications. *Chemical Society Reviews*. 2016;45(21):5925-50.
4. Hall PJ, Mirzaei M, Fletcher SI, Sillars FB, Rennie AJR, Shitta-Bey GO, et al. Energy storage in electrochemical capacitors: designing functional materials to improve performance. *Energy & Environmental Science*. 2010;3(9):1238.
5. Simon P, Gogotsi Y. *Materials for electrochemical capacitors*. Nanoscience and Technology: Co-Published with Macmillan Publishers Ltd, UK; 2009. p. 320-9.
6. Wang G, Zhang L, Zhang J. A review of electrode materials for electrochemical supercapacitors. *Chem Soc Rev*. 2012;41(2):797-828.
7. Roy P, Berger S, Schmuki P. TiO₂ Nanotubes: Synthesis and Applications. *Angewandte Chemie International Edition*. 2011;50(13):2904-39.
8. Lee K, Mazare A, Schmuki P. One-Dimensional Titanium Dioxide Nanomaterials: Nanotubes. *Chemical Reviews*. 2014;114(19):9385-454.
9. Ge M-Z, Cao C-Y, Huang J-Y, Li S-H, Zhang S-N, Deng S, et al. Synthesis, modification, and photo/photoelectrocatalytic degradation applications of TiO₂ nanotube arrays: a review. *Nanotechnology Reviews*. 2016;5(1).
10. Peighambardoust NS, Khameneh Asl S, Mohammadpour R, Asl SK. Band-gap narrowing and electrochemical properties in N-doped and reduced anodic TiO₂ nanotube arrays. *Electrochimica Acta*. 2018;270:245-55.
11. Peighambardoust NS, Khameneh Asl S, Maghsoudi M. The effect of doping concentration of TiO₂ nanotubes on energy levels and its direct correlation with photocatalytic activity. *Thin Solid Films*. 2019;690:137558.
12. Wu H, Li D, Zhu X, Yang C, Liu D, Chen X, et al. High-performance and renewable supercapacitors based on TiO₂ nanotube array electrodes treated by an electrochemical doping approach. *Electrochimica Acta*. 2014;116:129-36.
13. Samsudin NA, Zainal Z, Lim HN, Sulaiman Y, Chang S-K, Lim Y-C, et al. Enhancement of Capacitive Performance in Titania Nanotubes Modified by an Electrochemical Reduction Method. *Journal of Nanomaterials*. 2018;2018:1-9.
14. Stejskal J, Kratochvíl P, Jenkins AD. The formation of polyaniline and the nature of its structures. *Polymer*. 1996;37(2):367-9.
15. Cirić-Marjanović G. Recent advances in polyaniline research: Polymerization mechanisms, structural aspects, properties and applications. *Synthetic Metals*. 2013;177:1-47.
16. Nicolas-Debarnot D, Poncin-Epaillard F. Polyaniline as a new sensitive layer for gas sensors. *Analytica Chimica Acta*. 2003;475(1-2):1-15.
17. Xiao T, Wang X, Wang X, Li Z, Zhang L, Lv P, et al. Effects of monomer solvent on the supercapacitance performance of PANI/TiO₂ nanotube arrays composite electrode. *Materials Letters*. 2018;230:245-8.
18. Zhao S, Chen Y, Zhao Z, Jiang L, Zhang C, Kong J, et al. Enhanced capacitance of TiO₂ nanotubes topped with nanograss by H₃PO₄ soaking and hydrogenation doping. *Electrochimica Acta*. 2018;266:233-41.
19. Xing J, Zhang W, Yin M, Zhu X, Li D, Song Y. Electrodeposition of polyaniline in long TiO₂ nanotube arrays for high-areal capacitance supercapacitor electrodes. *Journal of Solid State Electrochemistry*. 2017;21(8):2349-54.
20. Faraji M. Interlaced polyaniline/carbon nanotube nanocomposite co-electrodeposited on TiO₂ nanotubes/Ti for high-performance supercapacitors. *Journal of Solid State Electrochemistry*. 2017;22(3):677-84.
21. Wang S, Xia Z, Li Q, Zhang Y. Fabrication of Polyaniline/Self-Doped TiO₂Nanotubes Hybrids as Supercapacitor Electrode by Microwave-Assisted Chemical Reduction and Electrochemical Deposition. *Journal of The Electrochemical Society*. 2017;164(13):D901-D7.
22. Gvozdenovic M, Jugovic B, Stevanovic J, Grgur B. Electrochemical synthesis of electroconducting polymers. *Chemical Industry*. 2014;68(6):673-84.
23. Lu Z, Yip C-T, Wang L, Huang H, Zhou L. Hydrogenated TiO₂Nanotube Arrays as High-Rate Anodes for Lithium-Ion Microbatteries. *ChemPlusChem*. 2012;77(11):991-1000.
24. Shao Q, Wang Y, Ge S, Bao L, Yang M, Zhu Y. Electrodeposition Synthesis of Polyaniline-Modified TiO₂Nanotube Arrays with Enhanced Photoelectrochemical Property. *Transactions of the Indian Ceramic Society*. 2015;74(3):152-6.
25. Hashemi Monfared A, Jamshidi M. Synthesis of polyaniline/titanium dioxide nanocomposite (PANI/TiO₂) and its application as photocatalyst in acrylic pseudo paint for benzene removal under UV/VIS lights. *Progress in Organic Coatings*. 2019;136:105257.
26. Lai L, Yang H, Wang L, Teh BK, Zhong J, Chou H, et al. Preparation of Supercapacitor Electrodes through Selection of Graphene Surface Functionalities. *ACS Nano*. 2012;6(7):5941-51.
27. Lasia A. *Semiconductors and Mott-Schottky Plots. Electrochemical Impedance Spectroscopy and its Applications*: Springer New York; 2013. p. 251-5.
28. Xie K, Li J, Lai Y, Zhang Za, Liu Y, Zhang G, et al. Polyaniline nanowire array encapsulated in titania nanotubes as a superior

electrode for supercapacitors. *Nanoscale*. 2011;3(5):2202.

29. Chen J, Xia Z, Li H, Li Q, Zhang Y. Preparation of highly capacitive polyaniline/black TiO₂ nanotubes as supercapacitor electrode by hydrogenation and electrochemical deposition. *Electrochimica Acta*. 2015;166:174-82.

30. Appadurai T, Subramaniam C, Kuppasamy R, Karazhanov S, Subramanian B. Electrochemical Performance of Nitrogen-Doped TiO₂ Nanotubes as Electrode Material for Supercapacitor and Li-Ion Battery. *Molecules (Basel, Switzerland)*. 2019;24(16):2952.